Identification of Glutamic Acid 479 as the Gluzincin Coordinator of Zinc in FtsH (HflB)†

Naoya Saikawa, Koreaki Ito, and Yoshinori Akiyama*

Institute for Virus Research, Kyoto University, Sakyo-ku, Kyoto 606-8507, Japan

Received September 7, 2001; Revised Manuscript Received November 15, 2001

ABSTRACT: *Escherichia coli* FtsH (HflB) is a membrane-bound and ATP-dependent metalloprotease. Its cytoplasmic domain contains a zinc-binding motif, $H^{417}EXXH$, whose histidine residues have been shown to be functionally important. Although they are believed to be involved directly in zinc coordination, nothing is known about the third zinc ligand of this protease. Sequence alignment indicates that glutamic acid residues are conserved among the FtsH homologues at positions corresponding to Glu^{479} and Glu^{585} of *E. coli* FtsH. We replaced each of them by Gln, Asp, Lys, or Val. Mutations at position 479 compromised the proteolytic functions of FtsH in vivo. In vitro proteolytic activities of the E479Q, E479V, and E479D mutant enzymes were much lower than that of the wild-type protein and were significantly stimulated by a high concentration of zinc ion. These mutant proteins retained the wild-type levels of ATPase activities, and their trypsin susceptibilities as well as CD spectra were essentially indistinguishable from those of the wild-type protein, indicating that the mutations did not cause gross conformational changes in FtsH. They exhibited reduced zinc contents upon purification. From these results, we conclude that Glu^{479} is a zinc-coordinating residue.

FtsH, an ATP-dependent metalloprotease of *Escherichia coli*, has two N-terminally located transmembrane segments, which are followed by a cytoplasmic ATPase domain and a protease domain (*1*−*3*). FtsH degrades not only soluble proteins but also some integral membrane proteins (*4*, *5*), including the SecY subunit of protein translocase (*6*), subunit *a* of the H^+-ATPase (Fo*a*) (*7*), and the YccA protein of unknown function (*8*). SecY and Fo*a* are rapidly degraded only when they are in unassembled subunit states (*6*, *7*). It has been proposed that FtsH initiates processive proteolysis of a membrane protein from a cytoplasmic domain and that this degradation is accompanied by dislocation of the substrate into the cytoplasm where the active sites of FtsH reside (*9*). Membrane association is essential for FtsH to degrade membrane proteins (*3*, *10*). The AAA ATPase activities may have an essential role in the dislocation process in which unfolding and presentation to the proteolytic active site of substrate proteins may occur.

FtsH undergoes self-processing, in which seven amino acid residues are removed from its C-terminus (*11*). Mutational analyses of the self-cleavage reaction showed that FtsH has limited cleavage specificity; it preferentially cleaves the C-terminal side of either a hydrophobic residue or a positively charged residue (*11*). FtsH is an oligomeric enzyme, like other ATP-dependent proteases. The N-terminal membrane region is required for the homooligomerization, which is a prerequisite for the ATPase and the proteolytic activities (*3*, *10*, *12*). FtsH also forms a complex with another membrane protein complex HflK/HflC (HflKC) (*13*, *14*). HflKC was suggested to have a regulatory role against the proteolytic activities of FtsH, and it differentially affects the proteolysis of soluble and membrane-bound substrates (*8*).

The protease domain of FtsH contains a sequence, His^{417}-Glu-Ala-Gly-His, which conforms to the zinc-binding consensus motif (HEXXH) found in zinc metalloproteases. The two histidine residues in this motif are thought to act as zinc ligands while the glutamic acid residue is involved in the acid−base catalytic mechanism (*15*). In accordance with this notion, mutational alternations of Glu^{418} and His^{421} are known to completely abolish the proteolytic activity of FtsH (*16*, *17*). In addition, the in vitro proteolytic activity of FtsH is inhibited by a metal chelator, 2-phenanthroline, and stimulated by Zn^{2+} (*18*). Although these observations are in complete agreement with FtsH being a zinc metalloprotease, its third zinc-coordinating residue has not been identified. Most zinc metalloproteases with an HEXXH motif (zincin) are classified into two subgroups, metzincin and gluzincin (*19*). Metzincins have a conserved motif, HEXXHXXGXX-HD, in which His or Asp at the C-terminal end acts as the third ligand for zinc coordination. On the other hand, gluzincins have a zinc-coordinating glutamic acid residue at a site 18−72 residues C-terminal to the HEXXH motif (*15*).

In this study, we attempted to identify the third zinc-coordinating residue of FtsH. One of the two evolutionally conserved glutamic acid residues found in FtsH, Glu^{479}, was shown to be functionally important. Mutational alternations of this residue can lower the proteolytic activity as well as the zinc content of the enzyme. We propose that Glu^{479} is the third zinc-coordinating residue of FtsH.

† This work was supported by grants from the Ministry of Education, Culture, Sports, Science and Technology, Japan (to Y.A. and K.I.), and from CREST, Japan Science and Technology Corporation (to K.I.).

* To whom correspondence should be addressed. Telephone: +81-75-751-4040. Fax: +81-75-771-5699 or +81-75-761-5626. E-mail: yakiyama@virus.kyoto-u.ac.jp.

10.1021/bi015748o CCC: $22.00
Published on Web 01/16/2002

Table 1: Plasmids and Primers for the *ftsH* Mutants

Plasmids	Primers*	pSTD113 derivatives	pSTD120 derivatives	pSTD323 derivatives
WT		pSTD113 (ref.12)	pSTD120 (ref.12)	pSTD323
YEXXH	5'-GAATCGACGGCTTACTACGAAGCGGGTC-3'	pSTD316	pSTD318	
HEXXY	5'-CCACGAAGCGGGTTATGCGATTATCGG-3'	pSTD317	pSTD319	
KEXXK	5'-GAATCGACGGCTTACAAGG-AAGCGGGTAAGGCGATTATCGGTCG-3'			pKSR69
E479K	5'-GTGGTCGTCTGGCAAAAGAGATCATCTAC-3'	pKSR6	pKSR10	
E479D	5'-GTGGTCGTCTGGCAGATGAGATCATCTAC-3'	pKSR24	pKSR36	pKSR53
E479V	5'-GTGGTCGTCTGGCAGTTGAGATCATCTAC-3'	pKSR26	pKSR38	pKSR48
E479Q	5'-GTGGTCGTCTGGCACAGGAGATCATCTAC-3'	pKSR28	pKSR40	
E480D	5'-GTCGTCTGGCAGAAGATATCATCTACGGG-3'	pKSR66		
E480V	5'-GTCGTCTGGCAGAAGTGATCATCTACGGG-3'	pKSR67		
E585K	5'-CTCATGAAATATAAGACTATCGACGCACC-3'	pKSR8	pKSR12	
E585D	5'-CTCATGAAATATGATACTATCGACGCACC-3'	pKSR30	pKSR42	
E585V	5'-CTCATGAAATATGTGACTATCGACGCACC-3'	pKSR32	pKSR44	
E585Q	5'-CTCATGAAATATGTGACTATCGACGCACC-3'	pKSR34	pKSR46	

*Only one of a complementary pair is shown.

MATERIALS AND METHODS

Bacterial Strains and Media. *E. coli* K-12 strains AD368 (*ftsH1/F′lacI*^{q}) (*20*) and AR5090 (Δ*ftsH3*::*kan, sfhC21*) (*3*) were described previously.

L medium (*21*) containing chloramphenicol (20 μg/mL) and/or ampicillin (50 μg/mL) was used for growing plasmid-bearing cells.

Plasmids. pSTD323 [*ftsH*(Δ*TM*)-*his*$_6$-*myc*] was constructed by deleting a region corresponding to the N-terminal transmembrane region of FtsH from pSTD113 (*ftsH-his*$_6$-*myc*) using a QuickChange mutagenesis kit (Strategene) and a pair of primers (CAATTTCACACAGGAAACAGCTATGCGTCAAATGCAGGGCGGCGG and CCGCCGCCCTGCATTTGACGCATAGCTGTTTCCTGTGTGAAATTG). Plasmids encoding FtsH-His$_6$-Myc and FtsH(ΔTM)-His$_6$-Myc derivatives with an amino acid substitution at position 479 or 585 or in the HEXXH motif are listed in Table 1. They were constructed as follows. Each of the mutations was first introduced into the *ftsH* gene on pSTD401 (*12*) using the QuickChange mutagenesis kit and the primers shown in Table 1. Then, their 0.7 kilo base pair *Mlu*I−*Nru*I fragments were used to substitute for the corresponding regions of pSTD120 (*12*), pSTD113 (*12*), and pSTD323. pSTD113 and pSTD323 were derived from pBlueScript SK(−) (Stratagene) whereas pSTD120 was from pSC101. pKY248 (*22*) carried the *secY* gene under the control of the *lac* promoter.

Complementation Abilities. A plasmid to be tested was introduced into AD368 (*ftsH1/F′lacI*^{q}), and the resulting transformant cells were plated on an L agar plate containing 1 mM isopropyl β-D-thiogalactopyranoside and 1 mM cAMP. Bacterial growth was scored after 12 h of incubation at 30 or 42 °C.

Detection of FtsH Variants by Immunoblotting. Cells of AR5090 carrying an *ftsH* plasmid were grown at 37 °C to a mid-log phase, and the *lac* transcription was induced with 1 mM isopropyl β-D-thiogalactopyranoside for 2 h. A portion of the cultures (containing about 6×10^7 cells) was removed and mixed with the same volume of 10% trichloroacetic acid. Proteins were analyzed by SDS−PAGE[1] and immunoblotting with anti-FtsH (*23*), anti-σ^{32} (a gift of M. Kanemori), or anti-SecY (*24*) antibodies. Visualization and quantification were done by means of an ECL detection kit (Amersham Pharmacia Biotech) and a Fuji LAS1000 lumino-image analyzer.

Purification of FtsH and Its Variants. FtsH-His$_6$-Myc and its variants were purified from cells of AR5090 carrying pSTD113, pSTD316, pSTD317, pKSR6, pKSR24, pKSR26, or pKSR28 by Ni^{2+}−nitrilotriacetic acid−agarose affinity chromatography as described previously (*3*). The purified proteins were extensively dialyzed against dialysis buffer (10 mM Tris-HCl, pH 8.1, 5 mM $MgCl_2$, 10% glycerol, 0.5% Nonidet P-40, 10 mM 2-mercaptoethanol).

FtsH(ΔTM)-His$_6$-Myc and its derivatives were purified from cells of AR5090 carrying pSTD323, pKSR51, pKSR69, pKSR53, or pKSR48. The peak fractions of Ni^{2+}−nitrilotriacetic acid−agarose affinity chromatography were subjected to buffer exchange using a NAP-10 or NAP-25 desalting column (Amersham Pharmacia Biotech) equilibrated with buffer A (10 mM Tris-HCl, pH 8.1, 10% glycerol, 5 mM $MgCl_2$, 10 mM 2-mercaptoethanol) and to Mono Q column chromatography. The Mono Q column was washed with buffer A and eluted with a 0−2 M linear gradient of NaCl in the same buffer. The peak fractions, as detected by SDS−PAGE and Coomassie brilliant blue staining, were pooled and dialyzed against 10 mM Tris-HCl, pH 8.1, 10% glycerol, and 10 mM 2-mercaptoethanol that had been prepared zinc-free using plasticware and glassware prewashed with 1 M HCl.

In Vitro Proteolytic Activities of FtsH. To measure the FtsH's activity to degrade resorufin-labeled casein, purified FtsH derivatives (4.5 μg) were incubated with resorufin-labeled casein (40 μg; Roche Diagnostics K.K.) at 42 °C in buffer (200 μL) containing 50 mM Tris-HCl, pH 8.1, 5 mM $MgCl_2$, 10 mM 2-mercaptoethanol, 0.5% Nonidet P-40, and $ZnCl_2$ (0, 0.5, 25, or 600 μM) in the presence or absence of 2.5 mM ATP. A 35 μL portion of the reaction mixture was withdrawn at intervals and mixed with 19 μL of 10% trichloroacetic acid. After 10 min or more at 0 °C, samples were centrifuged, the supernatant was mixed with 2 volumes of 0.5 M Tris-HCl, pH 8.8, and absorbance at 595 nm was measured.

To measure the FtsH's activity to degrade SecY, purified SecY (final concentration, 2.7−3.7 μg/mL) and the FtsH-

[1] Abbreviation: PAGE, polyacrylamide gel electrophoresis.

His_6-Myc or its variants (final concentration, 37 μg/mL) were incubated at 37 °C in buffer containing 50 mM Tris-HCl, pH 8.1, 5 mM $MgCl_2$, 10 mM 2-mercaptoethanol, 0.5% Nonidet P-40, 0 or 3.3 mM ATP, and either $ZnCl_2$ or zinc acetate (0, 0.5, 25, or 600 μM). Samples were withdrawn at intervals and mixed with the same volume of 2× SDS sample buffer (*25*). Proteins were separated by 15% acrylamide−0.12% *N*,*N*′-methylenebis(acrylamide) SDS−PAGE (*26*) and detected by immunoblotting using anti-SecY serum.

Metal Quantitation. The purified preparations of FtsH-(ΔTM)-His_6-Myc and its variants were denatured by treatment with 3% perchloric acid at room temperature. The denatured protein (220−470 μg) in 25 μL was mixed with 475 μL of 0.1 mM 4-(2-pyridylazo)resorcinol (PAR) in 500 mM HEPES/KOH, pH 7.5, and absorbance at 500 nm was measured using a Beckman DU-600 spectrophotometer (*27*). Zinc standard solution (atomic absorbance grade; nacalai tesque) was used as a standard.

ATPase Activity Assay. ATPase activities of FtsH-His_6-Myc and its derivatives were assayed as described previously (*20*). Briefly, 60 μL of a sample containing 50−150 ng of purified protein, 50 mM Tris-HCl, pH 8.1, 5 mM $MgCl_2$, 25 μM zinc acetate, 10 mM 2-mercaptoethanol, 0.5% Nonidet P-40, and 1 mM ATP was incubated at 37 °C for 1 h. Then, it was mixed with 240 μL of the malacite green/poly(vinyl alcohol)/ammonium molybdate reagent and 30 μL of 34% sodium citrate. After 30 min at room temperature, absorbance at 660 nm was measured.

Trypsin Digestion of FtsH. Trypsin digestion was carried out essentially as described by Akiyama et al. (*23*). Purified FtsH-His_6-Myc and its derivatives (about 0.1 μg/mL) were treated with trypsin (0.5 μg/mL) at 0 °C in buffer containing 50 mM Tris-HCl, pH 8.1, 5 mM $MgCl_2$, 25 μM zinc acetate, 10 mM 2-mercaptoethanol, and 0.5% Nonidet P-40 in the presence or absence of 5 mM ATP. Samples were withdrawn at intervals, mixed with the same volume of 2× SDS sample buffer containing 2 mM phenylmethanesulfonyl fluoride and 6 mM *p*-toluenesulfonyl-L-lysine chloromethyl ketone hydrochloride, and incubated at 37 °C for 5 min. Proteins were separated by 16.1% acrylamide−0.12% *N*,*N*′-methylenebis-(acrylamide)-modified gel and visualized by Coomassie brilliant blue staining.

Circular Dichronism (*CD*). CD spectra of purified FtsH-(ΔTM)-His_6-Myc, FtsH(ΔTM/KEXXK)-His_6-Myc, FtsH-(ΔTM/E479D)-His_6-Myc, and FtsH(ΔTM/E479V)-His_6-Myc (about 0.2 μg/mL) were obtained in the wavelength range of 200−250 nm using circular dichroism spectropolarimeters (Jasco J-725). Ten scans were averaged for each sample. Measurements were carried out at room temperature using a 0.1 cm path-length quartz cell. Buffer (10 mM Tris-HCl, pH 8.1, 10% glycerol, 5 mM $MgCl_2$, and 10 mM 2-mercaptoethanol) alone was used as a control.

RESULTS

Identification of Conserved Glutamic Acid Residues in a C-Terminal Region of FtsH. FtsH does not have a sequence conserved in metzincin (HEXXHXXGXXH/D) but has several glutamic acid residues in the downstream of the HEXXH motif. Computer-aided amino acid sequence alignment of FtsH homologues (Figure 1) revealed that two glutamic acid residues are completely conserved at positions

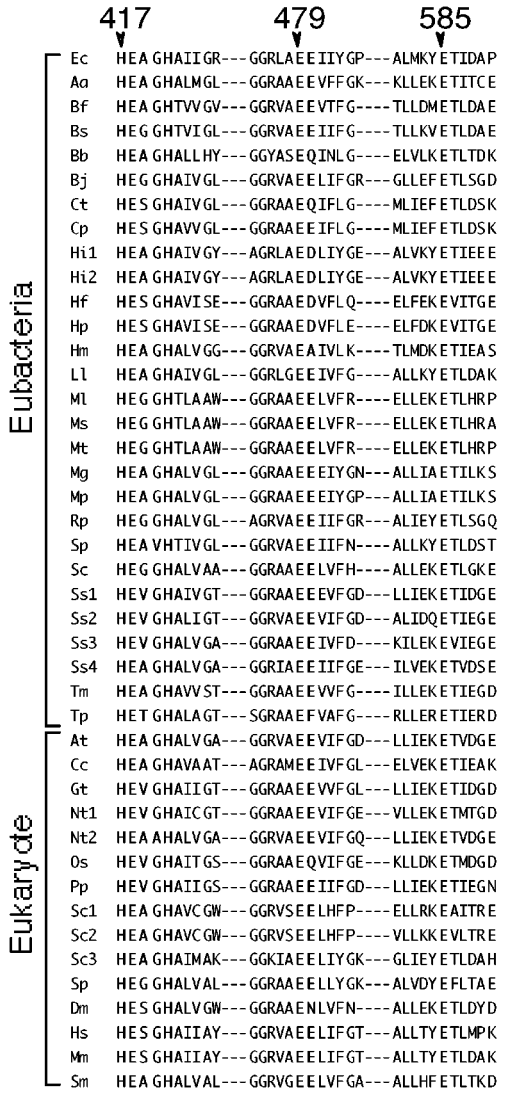

FIGURE 1: Sequence alignment for some selected intervals of FtsH homologues. Amino acid sequences of the FtsH homologues were aligned using the ClustalW program. The HEXXH motif and the conserved glutamic acid residues are shown in bold face, and only the sequences around them are shown. The positions of His^{417}, Glu^{479}, and Glu^{585} of *E. coli* FtsH are indicated by arrowheads. Abbreviations: Ec, *Escherichia coli* (accession number P28691); Aa, *Aquifex aeolicus* (AAC07029); Bf, *Bacillus firmus* (P94304); Bs, *Bacillus subtilis* (P37476); Bb, *Borrelia burgdorferi* (AAC67120); Bj, *Bradyrhizobium japonicum* (CAB51029); Ct, *Chlamydia trachomatis* (AAC68438); Cp, *Chlamydophila pneumon* (AAD19135); Hi1 and Hi2, *Haemophilus influenzae* [P71377(FtsH-a) and P45219-(FtsH-b)]; Hf, *Helicobacter felis* (O32617); Hp, *Helicobacter pylori* (P71408); Hm, *Heliobacillus mobili*s (AAC84037); Ll, *Lactococcus lactis* (P46469); Ml, *Mycobacterium leprae* (CAA18796); Ms, *Mycobacterium smegma*t (AAC32257); Mt, *Mycobacterium tuberculosis* (P96942); Mg, *Mycoplasma genitalium* (P47695); Mp, *Mycoplasma pneumoniae* (P75120); Rp, *Rickettsia prowazekii* (Q9ZEA2); Sp, *Streptococcus pneumoniae* (O69076); Sc, *Streptomyces coelicolor* (CAB42757); Ss1, Ss2, Ss3, and Ss4, *Synechocystis* sp. (Q55700, P73179, P73437, and P72991); Tm, T*hermotoga maritima* (AAD35665); Tp, *Treponema pallidum* (O83746); At, *Arabidopsis thaliana* (Q39102); Cc, *Cyanidium caldarium* (O19922); Gt, G*uillardia theta* (O78516); Nt1 and Nt2, *Nicotiana tabacum* [AAD17230(Pftf) and BAA33755]; Os, *Odontella sinensis* (P49825); Pp, *Porphyra purpurea* (P51327); Ss1, Ss2, and Ss3, *Saccharomyces cerevisiae* [S46611(YTA10), S54465-(YTA12), and P32795(YME1)]; Sp, *Schizosaccharomyces pombe* (CAA19064); Dm, *Drosophila melanogaster* (CAA19646); Hs, *Homo sapiens* (AAD20962); Mm, *Mus musculus* (AAC35558); Sm, *Schistosoma mansoni* (CAA82844).

corresponding to Glu[479] and Glu[585] in *E. coli* FtsH. These glutamic acids, the C-terminal 58th and 164th residues of the HEXXH motif, respectively, were investigated for their possible roles in the FtsH activities and zinc binding.

Complementation Activities of the Glu[479] and Glu[585] Variants. We constructed FtsH variants having either Asp (E479D, E585D), Val (E479V, E585V), Gln (E479Q, E585Q), or Lys (E479K, E585K) in place of Glu[479] or Glu[585]. Additionally, variants with alterations in the HEXXH motif were constructed by mutating conserved histidine(s) to Lys (KEXXK) and Tyr (YEXXH and HEXXY). All of the FtsH mutants carried a C-terminal polyhistidine and a Myc epitope tag (His_6-Myc tag) to facilitate their detection and purification. Abilities of the mutant genes to complement the *ftsH1*(Ts) mutation were examined. Expression of E585Q, E585D, and E479Q mutant genes from a low copy plasmid supported growth of the *ftsH1* mutant cells at restrictive temperature (42 °C), although slightly less efficiently than the *ftsH*$^+$ plasmid. On the other hand, neither of the E479K, E479D, E479V, E585K, E585V, HEXXY, or YEXXH mutant genes was active in the complementation.

In Vivo Proteolytic Function of the FtsH Variants. Although the *ftsH* gene function is essential for cell growth under the normal condition, the *sfhC21* suppressor mutation enables cells to grow without FtsH (*28*). Cells of AR5090 (Δ*ftsH sfhC21/F′lacZ*Δ*M15*) carrying the plasmid for the SecY-LacZα fusion protein form blue colonies on an agar plate containing 5-bromo-4-chloro-3-indolyl β-D-galactoside (Xg), because SecY-LacZα is stabilized in this strain. The extent of color development, which should be correlated with accumulation levels of SecY-LacZα (*6*), was used to assess the proteolytic activities of the FtsH variants that were coexpressed from a compatible plasmid. Thus, expression of wild-type FtsH as well as of E585K, E585D, E585Q, and E479Q mutants markedly decreased the color development. In contrast, cells expressing the E479K, E479D, E479V, E585V, YEXXH, and HEXXY forms of FtsH remained blue, suggesting that these FtsH variants had significantly impaired proteolytic function.

Their in vivo protease activities were studied more directly by examining cellular accumulation of a soluble and a membrane-bound substrate, σ^{32} and SecY, respectively, as well as the C-terminal self-processing of FtsH (Figure 2). The FtsH variants and SecY were expressed from compatible low copy plasmids in the Δ*ftsH* cells. Whereas wild-type FtsH-His_6-Myc was self-processed into FtsH′ that had lost the C-terminal His_6-Myc tag (Figure 2A, lane 11; *11*), no processing was observed for the proteolytically inactive YEXXH and HEXXY mutants (lanes 9 and 10). Although most Glu[585] mutants were self-processed (lanes 5−8), the E479Q and the E585V forms of FtsH were only less pronouncedly processed. No self-processed product was observed for E479K, E479D, and E479V (lanes 1−4), suggesting that these mutants lack the protease activity. Accumulation of σ^{32} and SecY was reduced markedly by expression of FtsH-His_6-Myc but not by expression of the HEXXH motif mutants (Figure 2B,C, lanes 9−11). Also, the E479K, E479D, E479V (lanes 1−3), and E585V (lane 7) mutants were unable to reduce these substrates. The E585K, E585D, E585Q, and E479Q mutants were apparently as active as the wild-type FtsH (lanes 4−6 and 8). Thus, the Glu[479] mutants were severely defective in the proteolytic functions. Glu[585] seemed less important since it was replaceable by several other amino acid residues.

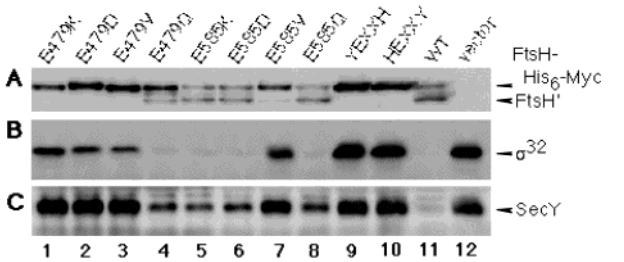

FIGURE 2: In vivo proteolytic functions of mutant enzymes with alteration at Glu[479] and Glu[585]. Cells of AR5090 (Δ*ftsH*) carrying two compatible plasmids, pKY248 (*secY*) and one of the plasmids encoding the *ftsH* derivatives as indicated below, were grown in L medium at 30 °C and induced with 1 mM isopropyl β-D-thiogalactopyranoside and 5 mM cAMP for 3 h for the synthesis of SecY and the FtsH variants. Proteins were precipitated by 5% trichloroacetic acid and analyzed by SDS−PAGE followed by immunoblotting using anti-FtsH (A), anti-σ^{32} (B), and anti-SecY (C) antibodies. The *ftsH* plasmids carried were pKSR10 [*ftsH*(*E479K*)-*his*$_6$-*myc*; lane 1], pKSR36 [*ftsH*(*E479D*)-*his*$_6$-*myc*; lane 2], pKSR38 [*ftsH*(*E479V*)-*his*$_6$-*myc*; lane 3], pKSR40 [*ftsH*(*E479Q*)-*his*$_6$-*myc*; lane 4], pKSR12 [*ftsH*(*E585K*)-*his*$_6$-*myc*; lane 5], pKSR42 [*ftsH*(*E585D*)-*his*$_6$-*myc*; lane 6], pKSR44 [*ftsH*(*E585V*)-*his*$_6$-*myc*; lane 7], pKSR46 [*ftsH*(*E585Q*)-*his*$_6$-*myc*; lane 8], pSTD318 [*ftsH*(*YEXXH*)-*his*$_6$-*myc*; lane 9], pSTD319 [*ftsH*(*HEXXY*)-*his*$_6$-*myc*; lane 10], pSTD120 [*ftsH-his*$_6$-*myc*; lane 11], and pMW119H (vector; lane 12). FtsH′ indicates the C-terminally self-processed product of FtsH-His_6-Myc (*11*).

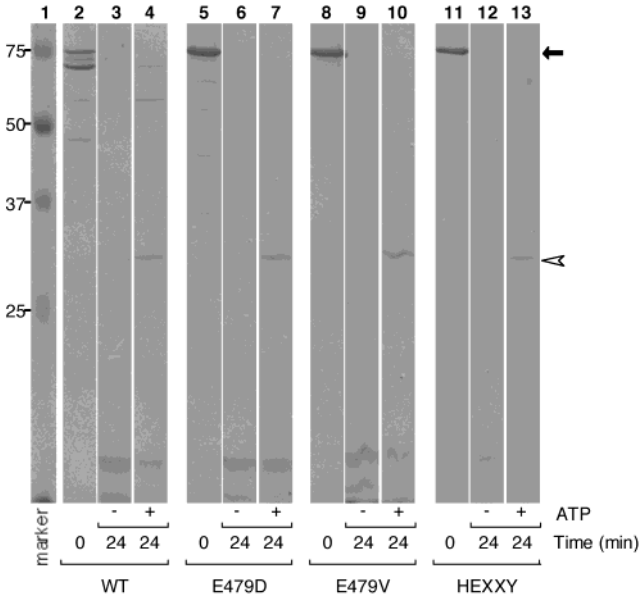

FIGURE 3: Nucleotide-induced conformational changes in the FtsH mutants. Purified samples of FtsH-His_6-Myc, FtsH(HEXXY)-His_6-Myc, FtsH(E479D)-His_6-Myc, and FtsH(E479V)-His_6-Myc (13 μg), as indicated, were treated with 5 μg/mL trypsin at 0 °C for 0 or 24 min in the presence or absence of 1 mM ATP. Proteins were separated by SDS−PAGE and stained with Coomassie brilliant blue. Positions of molecular mass markers (shown in kilodaltons) are indicated on the left. The arrow and open arrowhead indicate FtsH-His_6-Myc and the 33 kDa trypsin-resistant fragment generated in the presence of ATP, respectively.

Structural Integrity of the Glu[479] Mutants. It is known that gluzincins have a zinc-coordinating glutamate residue located at a site 18−72 residues C-terminal to the HEXXH motif. Our results raise a possibility that Glu[479] (the 58th residue from the HEXXH motif) serves as the third zinc ligand.

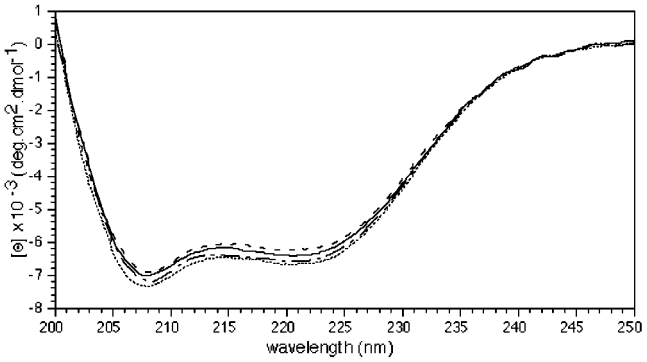

FIGURE 4: CD spectra of the FtsH(ΔTM) derivatives. CD spectra of FtsH(ΔTM)-His_6-Myc (—), FtsH(ΔTM/KEXXK)-His_6-Myc (— —), FtsH(ΔTM/E479D)-His_6-Myc (---), and FtsH(ΔTM/E479V)-His_6-Myc (— — -) were obtained as described in Materials and Methods.

To characterize the mutant enzymes biochemically, we purified the E479Q, E479D, E479V, E585D, and HEXXY variants as well as the wild-type FtsH protein. The purified FtsH(E479D)-His_6-Myc and FtsH(E479V)-His_6-Myc proteins retained significant ATPase activities. Although their ATPase activities were lower than that of the wild-type protein (about 40% and 70%, respectively, as compared with the wild-type enzyme), the significance of these levels of reduction is unclear since FtsH(E585D)-His_6-Myc and FtsH(HEXXY)-His_6-Myc also had reduced ATPase activities (about 33% and 45%, respectively, of wild type). To know whether the Glu^{479} alteration affected the overall structure of FtsH, we examined the trypsin digestion patterns of the purified proteins. It was shown that ATP binding induces some structural changes in FtsH, which can be demonstrated experimentally by the generation of a 33 kDa fragment upon trypsin treatment (*23*). However, an ATP-binding motif mutant does not undergo such a conformational change (*16*). As shown in Figure 3, the digestion profiles did not differ significantly between the WT and the mutant proteins. The digestion profiles upon shorter trypsin treatments did not significantly differ either among these proteins (data not shown). These results indicate that the mutations do not abolish the ATP-dependent conformational change of FtsH. We also constructed and purified soluble forms of these proteins, FtsH(ΔTM)-His_6-Myc, FtsH(ΔTM/E479D)-His_6-Myc, FtsH(ΔTM/E479V)-His_6-Myc, and FtsH(ΔTM/KEXXK)-His_6-Myc, which lacked the N-terminal membrane region. Their CD spectra were measured (Figure 4). The E479V,E479D, and KEXXK mutant proteins exhibited spectral profiles very similar to that of the wild-type FtsH-(ΔTM)-His_6-Myc; all of these proteins had about 22% α-helix, 20% β-sheet, and 25% β-turn. These results indicate that these mutations do not cause gross conformational changes in FtsH.

Increased Zinc Dependence of the Glu^{479} Mutant Enzymes. We examined in vitro proteolytic activities of the E479Q, E479D, and E479V mutant proteins (Figure 5). FtsH-His_6-Myc degraded resorufin-labeled casein very efficiently without addition of Zn^{2+} to the reaction buffer. Its activity remained unaffected by addition of Zn^{2+} up to 600 μM (Figure 5A). Thus, the wild-type FtsH-His_6-Myc may contain tightly bound zinc ions even after purification. In contrast, FtsH(E479D)-His_6-Myc (Figure 5B) and FtsH(E479V)-His-Myc (Figure 5C) showed very low casein-degrading activities in the zinc-free reaction buffer. Addition of Zn^{2+} significantly stimulated the proteolytic activities of these mutant proteins; casein-degradation activities of FtsH(E479Q)-His_6-Myc,

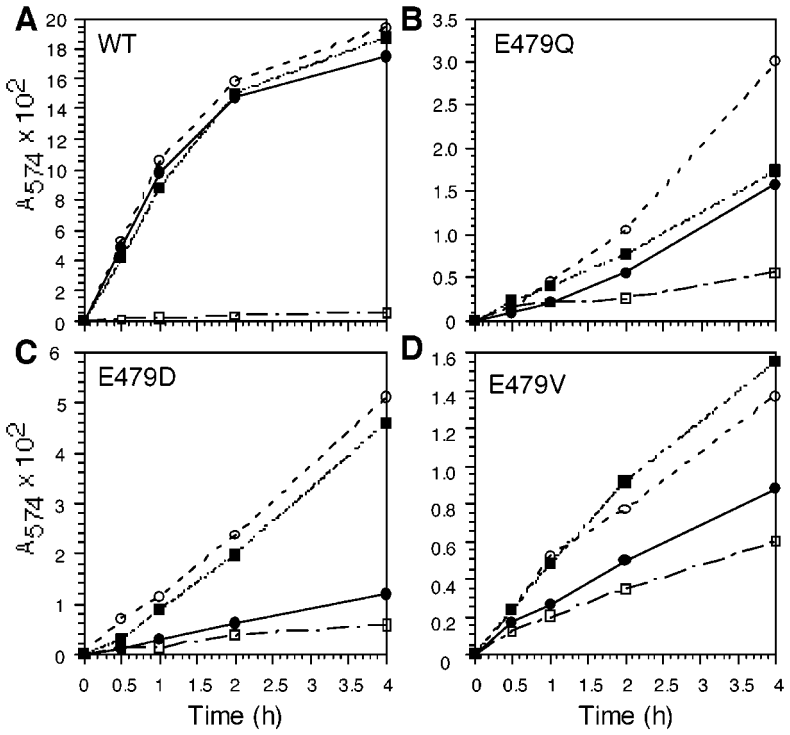

FIGURE 5: Degradation of resorufin-labeled casein by the FtsH variants. 4.5 μg each of FtsH-His_6-Myc (A), FtsH(E479Q)-His_6-Myc (B), FtsH(E479D)-His_6-Myc (C), and FtsH(E479V)-His_6-Myc (D) was incubated at 42 °C in a 200 μL reaction mixture with 40 μg of resorufin-labeled casein in the presence of 2.5 mM ATP (closed circles), 2.5 mM ATP and 25 μM $ZnCl_2$ (open circles), 2.5 mM ATP and 600 μM $ZnCl_2$ (closed squares), or 600 μM $ZnCl_2$ but no ATP (open squares). Samples were withdrawn at the indicated time points and mixed with trichloroacetic acid. After centrifugation, absorbance at 574 nm of the supernatants was measured.

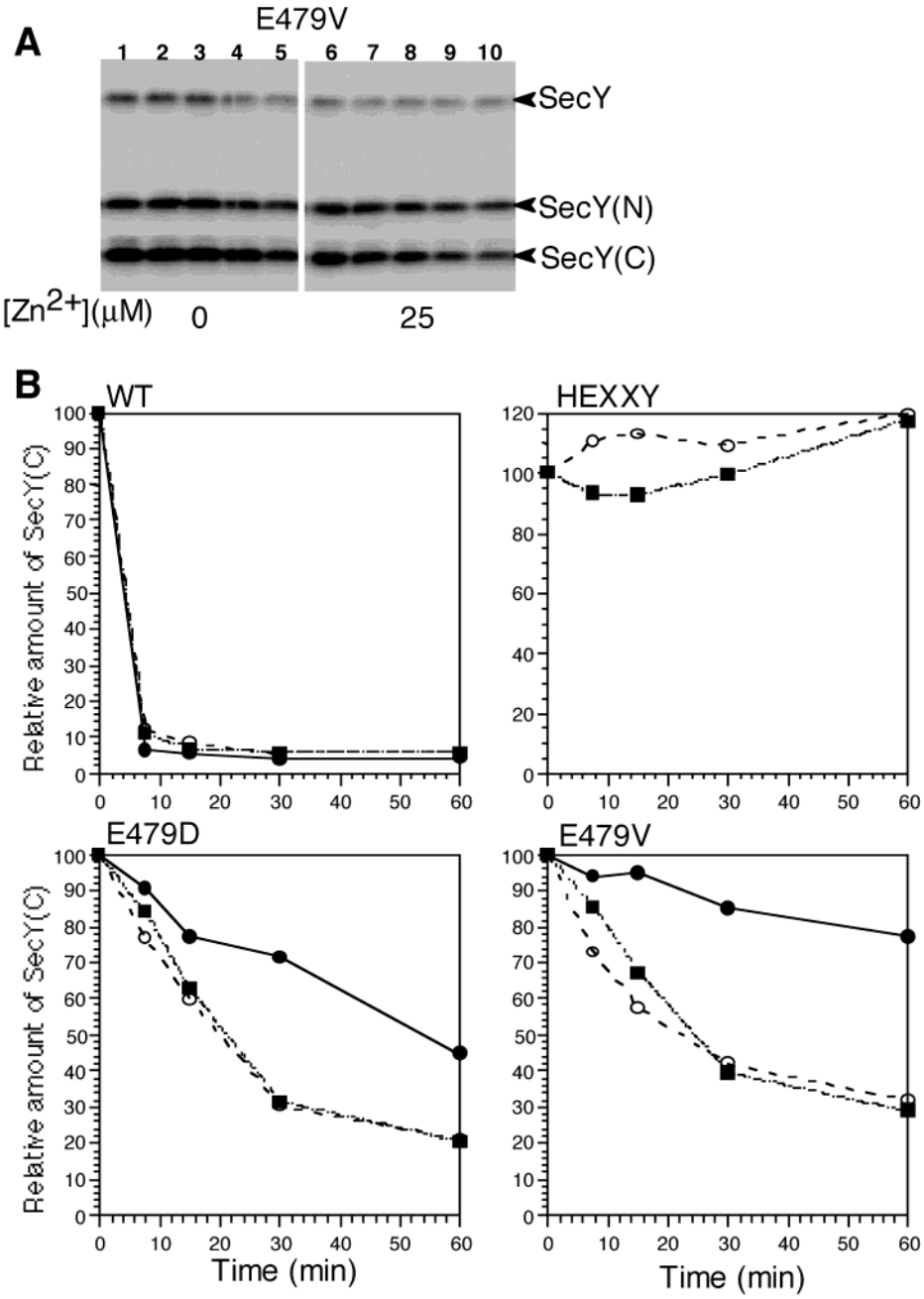

FIGURE 6: Degradation of SecY by the FtsH variants. (A) FtsH(E479V)-His_6-Myc (1.1 μg) was incubated at 37 °C in a 30 μL reaction mixture with SecY (53 ng) in the presence of 2.5 mM ATP and either 0 or 25 μM $ZnCl_2$. At the indicated time points, samples were withdrawn and analyzed by SDS−PAGE and immunoblotting using anti-SecY antibody. SecY, SecY(N), and SecY(C) indicate intact SecY, the N-terminal fragment of SecY, and the C-terminal fragment of SecY, respectively, present in the purified SecY preparation used in this experiment. (B) SecY degradation was followed in the presence of FtsH-His_6-Myc, FtsH(HEXXY)-His_6-Myc, FtsH(E479D)-His_6-Myc, or FtsH(E479V)-His_6-Myc (1.1 μg), in the presence of 2.5 mM ATP (open circles), 2.5 mM ATP plus 25 μM $ZnCl_2$ (closed circles), or 2.5 mM ATP plus 600 μM $ZnCl_2$ (closed squares). Intensities of the SecY(C) fragment were quantified, and relative values (% of the initial intensity) were plotted.

FtsH(E479D)-His_6-Myc, and FtsH(E479V)-His_6-Myc were stimulated 1.8-fold, 4.1-fold, and 1.5-fold, respectively, by 25 μM Zn^{2+}. All of the above reactions of casein degradation were ATP dependent (Figure 5). In the presence of 25 μM zinc, FtsH(E479Q)-His_6-Myc exhibited a 25-fold lower V_{max} (0.0057 μg mL^{-1} min^{-1}, with 22.5 μg of FtsH-His_6-Myc/mL) as compared with the wild-type protein (0.15 μg mL^{-1} min^{-1}), while the difference in the K_m values was much smaller (159 and 40 μg/mL, respectively), indicating that the mutation mainly affected the catalytic reaction.

To study proteolytic activities against SecY, FtsH was incubated with purified SecY, and its degradation was followed by immunoblotting. As described previously (*29*), the SecY preparation contained two fragments, SecY(N) and SecY(C), which had presumably been generated by OmpP after cell disruption (Figure 6A). Although appreciable fractions of the intact SecY aggregate into SDS-resistant forms upon incubation at 37 °C, SecY(N) and SecY(C) do not (*10*). Thus, decrease of these fragments, rather than that of intact SecY, was taken as the result of proteolysis. Again,

FtsH-His_6-Myc-mediated proteolysis of SecY(C) was independent of the Zn^{2+} concentration in the reaction mixture (Figure 6). FtsH(E479D)-His_6-Myc- and FtsH(E479V)-His_6-Myc-dependent SecY(C) degradation, which was very slow in the absence of Zn^{2+}, was accelerated by Zn^{2+} inclusion in the buffer (Figure 6B). FtsH(E479K)-His_6-Myc and FtsH(E479Q)-His_6-Myc also showed similar zinc dependence in their SecY-degrading activities (data not shown). The HEXXY mutant protein showed no proteolytic activity even in the presence of added zinc (Figure 6B).

Decreased Metal Contents of the Glu^{479} Mutants. Metal contents of FtsH(ΔTM)-His_6-Myc, FtsH(ΔTM/E479D)-His_6-Myc, FtsH(ΔTM/E479V)-His_6-Myc, and FtsH(ΔTM/KEXXK)-His_6-Myc were measured spectrophotometrically using 4-(2-pyridylazo)resorcinol (PAR). The value for FtsH(ΔTM)-His_6-Myc was 0.92 M metal ion/M protein, suggesting that each FtsH molecule contains one metal ion. In contrast, FtsH(ΔTM/KEXXK)-His_6-Myc contained only 0.13 M metal ion/M protein, confirming the importance of the HEXXH motif in metal binding. The values for FtsH(ΔTM/E479D)-His_6-Myc and FtsH(ΔTM/E479V)-His_6-Myc were 0.72 and 0.50, respectively. Thus, we observed reduced zinc contents for the Glu^{479} mutant proteins.

DISCUSSION

The HEXXH zinc metalloproteases have three residues that are directly involved in coordination of the zinc ion; two of them are histidine residues within the HEXXH motif and the remaining Glu (in gluzincin) or His/Asp (in metzincin) is located in the C-terminal side of this motif (*15*). No information has been available for the third Zn^{2+} ligand of FtsH. Here we show that Glu^{479} of FtsH is completely conserved among the FtsH homologues from prokaryotes to higher organisms. Our results suggest that Glu^{479} of FtsH is the third ligand for zinc coordination. First, the Glu^{479} alterations to Lys, Asp, and Val severely compromised the in vivo proteolytic activities. Second, the purified mutant enzymes lacked the activities to degrade resorufin-labeled casein and SecY unless supplemented with Zn^{2+} exogenously. Third, these mutant proteins had reduced metal contents. Finally, trypsin digestion profiles as well as CD spectra indicated that substitutions of Glu^{479} did not cause gross conformational changes. Herman et al. (*30*) suggested that the *ftsH1*(Ts) mutation impairs the zinc binding of FtsH. This mutation causes amino acid substitutions at two positions, and one of them (Glu^{466} to Leu) is close to Glu^{479}. The *ftsH1* mutation might affect the local conformation of the zinc-binding region. Formally, a possibility has not been ruled out that Glu^{479} is not directly coordinating zinc and that its substitution interferes with zinc coordination. However, we do not favor this possibility as an Asp or Val replacement of the adjacent Glu^{480} residue, which is also conserved in many of the FtsH homologues, did not affect the FtsH functions (data not shown).

We found another conserved residue, Glu^{585}, in the FtsH homologues. However, its mutational changes were largely silent except for E585V. Glu^{585} is located near the C-terminal end of an α-helical coiled-coil motif, which has been proposed to be functionally important in FtsH (*31*). The E585V mutant might disturb this region. Exact roles of this motif and the Glu^{585} residue await further clarification.

Substitutions of Glu^{479} did not entirely abolish the proteolytic activity of FtsH. Cummins et al. (*32*) suggested that metalloproteases with a longer spacer between the second and third ligands have a more flexible zinc-coordinating sphere and are more tolerant to substitutions of the third zinc ligand. Thus, an Asp substitution for the third zinc-coordinating residue that is 59 amino acids away from the HEXXH motif only partially inactivates EP24.11 (*33*), whereas the same Glu to Asp substitution at the third ligand that is only 25 or 24 residues away from the second ligand inactivated EP24.15 (*32*) and ACE C (*34*) completely. FtsH might have a flexible zinc-coordinating sphere, as its third ligand (Glu^{479}) is separated from the HEXXH motif by 58 amino acid residues. It should be noted, however, that aminopeptidase A has a short (19 residues) distance between the second ligand and the third ligand, which can be mutated to Asp with only ~40% reduction in the enzymatic activity (*35*). Thus, we do not understand completely the different requirements for the third zinc ligand observed in different zinc metalloproteases.

The E479D and E479V mutant proteins had very low in vitro proteolytic activities although our quantitation showed that they still had 50−70% metal content. It seems possible that these mutant enzymes have abnormal positioning of the active site zinc caused by the substitutions of the third ligand residue, and this results in the low enzymatic activities. We have shown previously that several mutant forms of FtsH, including FtsH(HEXXY),[2] dominantly interfere with the proteolytic activity of the wild-type protein by forming a mixed complex in vivo (*3*, *36*). Assuming the heterogeneous presence of zinc-free (inactive) and zinc-containing (partially active) mutant proteins, lower proteolytic activities of the Glu^{479} mutant might be explained by the mixed oligomer formation, in which the negative effect may be exaggerated. The E479D protein had higher proteolytic activity and metal content than the E479V protein. Probably an acidic side chain is less disturbing the zinc coordination than a hydrophobic side chain at this position.

ACKNOWLEDGMENT

We thank M. Kanemori for anti-σ^{32}, S. Kitada for useful suggestions in metal quantitation, H. Mori, S. Chiba, K. Kanehara, and N. Shimohata for discussion, and M. Yamada, M. Sano, Y. Shimizu, and K. Mochizuki for technical assistance.

REFERENCES

1. Tomoyasu, T., Yamanaka, K., Murata, K., Suzaki, T., Bouloc, P., Kato, A., Niki, H., Hiraga, S., and Ogura, T. (1993) *J. Bacteriol. 175*, 1352−1357.
2. Tomoyasu, T., Yuki, T., Morimura, S., Mori, H., Yamanaka, K., Niki, H., Hiraga, S., and Ogura, T. (1993) *J. Bacteriol. 175*, 1344−1351.
3. Akiyama, Y., and Ito, K. (2000) *EMBO J. 19*, 3888−3895.
4. Akiyama, Y., and Ito, K. (1998) in *Handbook of Proteolytic Enzymes* (Barret, A. J., Rawlings, N. D., and Woessner, J. F., Eds.) pp 1502−1504, Academic Press, London, U.K.
5. Langer, T. (2000) *Trends Biochem. Sci. 25*, 247−251.
6. Kihara, A., Akiyama, Y., and Ito, K. (1995) *Proc. Natl. Acad. Sci. U.S.A. 92*, 4532−4536.

[2] Y. Akiyama, unpublished results.

7. Akiyama, Y., Kihara, A., and Ito, K. (1996) *FEBS Lett. 399*, 26−28.
8. Kihara, A., Akiyama, Y., and Ito, K. (1998) *J. Mol. Biol. 279*, 175−188.
9. Kihara, A., Akiyama, Y., and Ito, K. (1999) *EMBO J. 18*, 2970−2981.
10. Akiyama, Y., and Ito, K. (2001) *Biochemistry 40*, 7687−7693.
11. Akiyama, Y. (1999) *Biochemistry 38*, 11693−11699.
12. Akiyama, Y., Yoshihisa, T., and Ito, K. (1995) *J. Biol. Chem. 270*, 23485−23490.
13. Kihara, A., Akiyama, Y., and Ito, K. (1996) *EMBO J. 15*, 6122−6131.
14. Akiyama, Y., Kihara, A., Mori, H., Ogura, T., and Ito, K. (1998) *J. Biol. Chem. 273*, 22326−22333.
15. Rawlings, N. D. (1998) in *Handbook of Proteolytic Enzymes* (Barret, A. J., Rawlings, N. D., and Woessner, J. F., Eds.) pp 989−991, Academic Press, London, U.K.
16. Karata, K., Inagawa, T., Wilkinson, A. J., Tatsuta, T., and Ogura, T. (1999) *J. Biol. Chem. 274*, 26225−26232.
17. Qu, J.-N., Makino, S., Adachi, H., Koyama, Y., Akiyama, Y., Ito, K., Tomoyasu, T., Ogura, T., and Matsuzawa, H. (1996) *J. Bacteriol. 178*, 3457−3461.
18. Tomoyasu, T., Gamer, J., Bukau, J., Kanemori, M., Mori, H., Rutman, A. J., Oppenheim, A. B., Yura, T., Yamanaka, K., Niki, H., Hiraga, S., and Ogura, T. (1995) *EMBO J. 14*, 2551−2560.
19. Hooper, N. M. (1994) *FEBS Lett. 354*, 1−6.
20. Akiyama, Y., Kihara, A., Tokuda, H., and Ito, K. (1996) *J. Biol. Chem. 271*, 31196−31201.
21. Silhavy, T. J., Berman, M. L., and Enquist, L. W. (1984) *Experiments with Gene Fusions*, Cold Spring Harbor Laboratory Press, Cold Spring Harbor, NY.
22. Taura, T., Baba, T., Akiyama, Y., and Ito, K. (1993) *J. Bacteriol. 175*, 7771−7775.
23. Akiyama, Y., Ehrmann, M., Kihara, A., and Ito, K. (1998) *Mol. Microbiol. 28*, 803−812.
24. Shimoike, T., Taura, T., Kihara, A., Yoshihisa, T., Akiyama, Y., Cannon, K., and Ito, K. (1995) *J. Biol. Chem. 270*, 5519−5526.
25. Laemmli, U. K. (1970) *Nature 227*, 680−685.
26. Akiyama, Y., and Ito, K. (1985) *EMBO J. 4*, 3351−3356.
27. Bell, J., and Ash, D. E. (1997) *Biochemistry 36*, 16239−16246.
28. Ogura, T., Inoue, K., Tatsuta, T., Suzaki, T., Karata, K., Young, K., Su, L.-H., Fierke, C. A., Jackman, J. E., Raetz, C. R. H., Coleman, J., Tomoyasu, T., and Matsuzawa, H. (1999) *Mol. Microbiol. 31*, 833−844.
29. Matsuo, E., Sampei, G., Mizobuchi, K., and Ito, K. (1999) *FEBS Lett. 461*, 6−8.
30. Herman, C., Lecat, S., D'Ari, R., and Bouloc, P. (1995) *Mol. Microbiol. 18*, 247−255.
31. Shotland, Y., Teff, D., Koby, S., Kobiler, O., and Oppenheim, A. B. (2000) *J. Mol. Biol. 299*, 963−964.
32. Cummins, P. M., Pabon, A., Margulies, E. H., and Glucksman, M. J. (1999) *J. Biol. Chem. 274*, 16003−16009.
33. Le Moual, H., Devault, A., Roques, B. P., Crine, P., and Boileau, G. (1991) *J. Biol. Chem. 266*, 15670−15674.
34. Williams, T. A., Corvol, P., and Soubrier, F. (1994) *J. Biol. Chem. 269*, 29430−29434.
35. Vazeux, G., Wang, J., Corvol, P., and Llorens-Cortès, C. (1996) *J. Biol. Chem. 271*, 9069−9074.
36. Akiyama, Y., Shirai, Y., and Ito, K. (1994) *J. Biol. Chem. 269*, 5225−5229.

BI015748O